

Impact of Ion-Irradiation upon Microstructure and Magnetic Properties of NANOPERM-Type $\text{Fe}_{81}\text{Mo}_8\text{Cu}_1\text{B}_{10}$ Metallic Glass

M. HASIAK^{a,*} AND M. MIGLIERINI^{b,c}

^aWrocław University of Science and Technology, Department of Mechanics and Materials Science Engineering, Smoluchowskiego 25, 50-370 Wrocław, Poland

^bSlovak University of Technology in Bratislava, Institute of Nuclear and Physical Engineering, Ilkovičova 3, 812 19 Bratislava, Slovakia

^cCzech Technical University in Prague, Department of Nuclear Reactors, V Holešovičkách 2, 180 00 Prague, Czech Republic

Microstructure and soft magnetic properties of the $\text{Fe}_{81}\text{Mo}_8\text{Cu}_1\text{B}_{10}$ amorphous alloy in the as-quenched state and after irradiation with N^+ ions are investigated. CEMS spectra show that the irradiated surface at the air side of the ribbons was significantly affected. On the other hand, no noticeable changes were observed at the opposite wheel side. More deep subsurface regions are also not altered as evidenced by CXMS spectra. Thermomagnetic measurements have shown presence of two magnetically different phases with well distinguished Curie points. They can be ascribed to the amorphous matrix and crystalline phases. The latter were quenched-in during the production process and/or induced by ion bombardment. Curie temperatures of the amorphous matrixes were calculated using the Heisenberg model. For the as-quenched and irradiated ribbons they are of 223 K and 228 K, respectively. The behaviour of coercivity versus temperature was also analysed.

DOI: [10.12693/APhysPolA.133.680](https://doi.org/10.12693/APhysPolA.133.680)

PACS/topics: 75.50.Bb, 75.60.Ej, 75.30.Kz, 61.80.-x, 76.80.+y

1. Introduction

Fe-based metallic glasses are very interesting because they exhibit unique combination of soft magnetic properties [1]. Magnetic materials with the Curie point close to the room temperature are attractive since magnetocaloric effect observed in these alloys gives possibility to use them in magnetic refrigerators [2]. From the other side, magnetic properties are strongly related to the microstructure. Therefore, understanding the role of microstructural changes of metallic glasses caused by heat treatment or other effects (including ion irradiation) upon their soft magnetic properties is still in the centre of interest of many researchers [3–5].

In this paper, we present the results of microstructural investigations performed upon the $\text{Fe}_{81}\text{Mo}_8\text{Cu}_1\text{B}_{10}$ metallic glass in the as-quenched state and after irradiation with N^+ ions to the total fluence of 2×10^{16} ions/cm². In doing so, we have employed Mössbauer spectroscopy and thermomagnetic characteristics such as temperature dependence of magnetization and hysteresis loops.

2. Experimental procedure

Fe-based metallic glass with the nominal composition of $\text{Fe}_{81}\text{Mo}_8\text{Cu}_1\text{B}_{10}$ was prepared by the method of pla-

nar flow casting of a melt upon quenching wheel in the air. Iron enriched by the stable isotope ^{57}Fe to about 50% was used to enhance the sensitivity of Mössbauer effect investigations. The resulting ribbons were about 20 μm thick and 1 ÷ 2 mm wide. They were bombarded with N^+ ions of 130 keV energy into their air (shiny) side to the total fluency of 2×10^{16} ions/cm². This energy was chosen intentionally because it provides maximum penetration depth of N^+ ions of about 148 nm. Thus, majority of the deposited ions are located within the screening depth of Conversion Electron Mössbauer Spectrometry (CEMS) which is about 200 nm. In addition, Conversion X-ray Mössbauer Spectrometry (CXMS) was also applied. It scans subsurface regions to the depth of about 5 μm . Room temperature Mössbauer spectra were recorded using a constant acceleration mode with a $^{57}\text{Co}(\text{Rh})$ gamma source. Velocity scale was calibrated with respect to a room temperature Mössbauer spectrum of *bcc*-Fe foil. The obtained data were evaluated using the CONFIT software. Thermomagnetic characteristics were recorded in the temperature range 50–400 K and external magnetic field up to 50 mT to analyse soft magnetic properties of the studied samples. Magnetic measurements were performed using a VersaLab system (Quantum Design).

3. Results and discussion

CEMS spectra of the as-quenched ribbons in Fig. 1a and 1c present intensive central broad lines which are

*corresponding author; e-mail: Mariusz.Hasiak@pwr.edu.pl

ascribed to the amorphous parts of the samples. In addition, sextuplet-like features are also observed. They identify a presence of crystalline components. Namely, *bcc*-Fe and magnetite (Fe_3O_4) were unveiled. It is noteworthy that the latter is seen only at the wheel side of the ribbon (Fig. 1c). The crystallites were formed during the production of the ribbons.

After the irradiation, the amount of *bcc*-Fe at the air side, which was exposed to irradiation, has increased from 7% in the as-quenched state to 28%. In addition, formation of crystalline nitrides was also confirmed and they have reached also about 28%. Identification of the nitrides is not straightforward because the linewidths of their sextets are quite broad (~ 0.55 mm/s) which suggests structural disorder. The obtained hyperfine magnetic fields of 28.9, 25.5, and 23.9 T are close to those of FeI and FeII in $\varepsilon\text{-Fe}_2\text{N}_x$ [6]. The total contribution of crystallites at the wheel side before and after the irradiation was almost unchanged (29%, resp. 30%). This is not surprising as all implanted N^+ ions were stopped in a vicinity of the air side and they were unable to reach deeper places than ~ 150 nm.

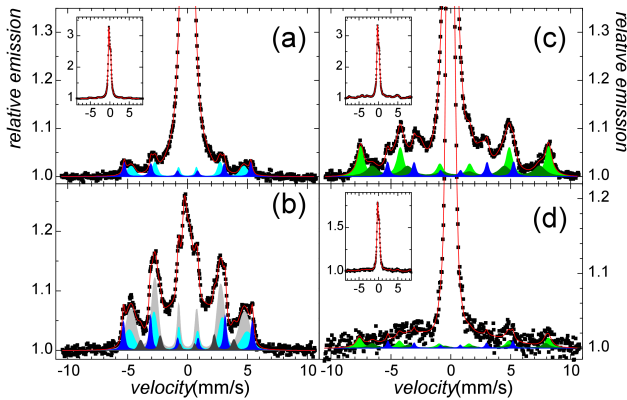


Fig. 1. Room temperature CEMS spectra of the $\text{Fe}_{81}\text{Mo}_8\text{Cu}_1\text{B}_{10}$ alloy taken from the air (a,b) and wheel (c,d) sides of the ribbons in the as-quenched state (a,c) and after irradiation with 2×10^{16} ions/ cm^2 (b,d). The insets show full spectra. Spectral components that belong to crystalline phases are given in colour: *bcc*-Fe with its interfacial regions (blue and cyan), magnetite Fe_3O_4 (A sites – light green, B sites – dark green), nitrides (shades of grey).

The amorphous phase at the air side of the as-quenched alloy is paramagnetic with an average quadrupole splitting ~ 0.41 mm/s. After irradiation, very minute decrease (in the error range) to 0.39 mm/s is observed. At the same time, its relative content decreases from 84% to 18% and magnetically active regions (26%) occur. The latter are formed by polarization via ferromagnetic exchange interactions among nitrides. At the wheel side, no changes in the amorphous phase are observed before and after irradiation with CEMS.

Situation in deeper subsurface region is documented by the help of CXMS spectra in Fig. 2. Only small amounts of *bcc*-Fe (6% and 10% for the air and wheel

side, respectively) are seen in the as-quenched alloy. No traces of magnetite were found in these deeper regions.

After irradiation, the total amount of *bcc*-Fe and nitrides has decreased to about 49% at the air side. The wheel side is completely amorphous and paramagnetic.

Presence of crystallites in the as-quenched as well as irradiated samples suggests more complex magnetic structure. This is evidenced by Fig. 3 where magnetization versus temperature curves recorded in zero-field (ZFC) and field cooled (FC) mode for the $\text{Fe}_{81}\text{Mo}_8\text{Cu}_1\text{B}_{10}$ alloy in the as-quenched state and after irradiation measured at external DC magnetic field of 10 mT are presented. In both modes, the magnetization monotonically decreases with temperature of measurements for all investigated samples. It is noteworthy that none of the magnetization curves drops down to zero which implies multiphase natures of the samples. This was confirmed by Mössbauer effect measurements which have confirmed coexistence of amorphous and crystalline phases. Even though the CEMS and CXMS techniques scan only surface regions (which eventually extend down to about $5 \mu\text{m}$) this structural diversity affects also bulk properties as evidenced by the magnetization curves in Fig. 3.

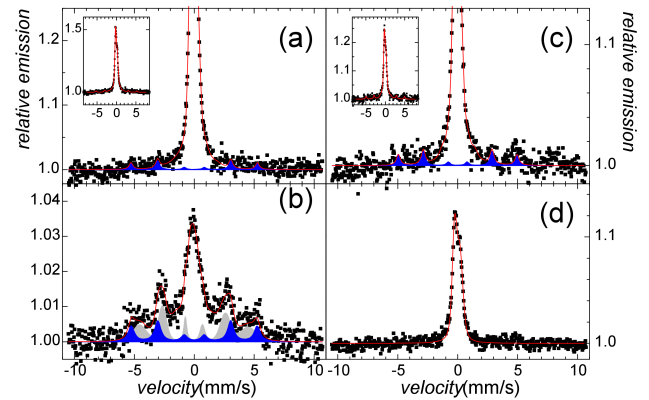


Fig. 2. Room temperature CXMS spectra of the $\text{Fe}_{81}\text{Mo}_8\text{Cu}_1\text{B}_{10}$ alloy taken from the air (a,b) and wheel (c,d) sides of the ribbons in the as-quenched state (a,c) and after irradiation with 2×10^{16} ions/ cm^2 (b, d). The insets show full spectra. Spectral components that belong to crystalline *bcc*-Fe and nitrides are plotted in blue and light grey, respectively.

After irradiation, the magnetization decreases for both ZFC and FC modes as compared with that of the as-quenched alloy. This decrease is caused by occurrence of structural defects due to irradiation-induced formation of crystallites. $M(T)$ curves recorded in the FC mode exhibit slightly higher values than those taken in the ZFC mode. This behaviour is visible both for non-irradiated (as-quenched) and irradiated $\text{Fe}_{81}\text{Mo}_8\text{Cu}_1\text{B}_{10}$ samples.

The Curie temperature of the amorphous matrix T_C^{am} for the as-quenched and irradiated alloys were derived using the Heisenberg model [7]. As demonstrated in Fig. 4, the obtained T_C^{am} values equal to 223 K and 228 K, respectively. Slight increase in T_C^{am} of the irradiated sample is presumably caused by the presence of

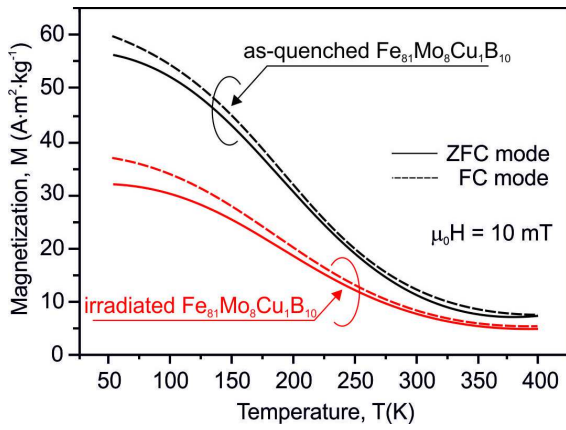


Fig. 3. Temperature dependence of magnetization for the $\text{Fe}_{81}\text{Mo}_8\text{Cu}_1\text{B}_{10}$ alloy in the as-quenched state and after irradiation with 2×10^{16} ions/ cm^2 recorded in zero-field cooled (solid line) and field cooled (dash line) mode at external magnetic field of 10 mT.

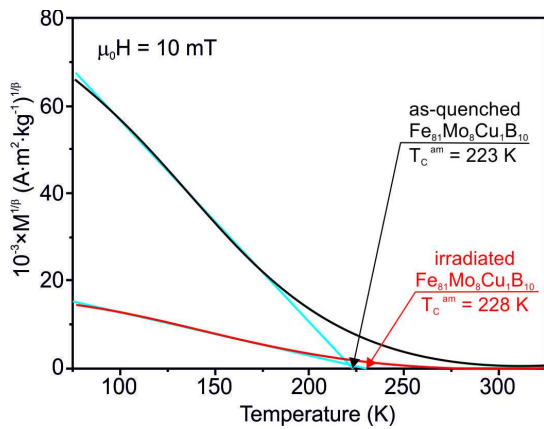


Fig. 4. Zero-field cooling $M^{1/\beta}$ ($\beta = 0.36$) as a function of temperature for the $\text{Fe}_{81}\text{Mo}_8\text{Cu}_1\text{B}_{10}$ alloy in the as-quenched state and after irradiation with 2×10^{16} ions/ cm^2 .

crystalline phases that through ferromagnetic exchange interactions polarize also the residual amorphous matrix. Even though the crystallites were identified predominantly in the near-surface regions they considerably affect also the bulk of the ribbons.

Figure 5 introduces hysteresis loops for the $\text{Fe}_{81}\text{Mo}_8\text{Cu}_1\text{B}_{10}$ alloy irradiated with 2×10^{16} ions/ cm^2 which were measured at temperatures of 50, 150, and 250 K. All characteristics were recorded for the maximum external DC magnetic field of 50 mT. As it can be seen the magnetization decreases with temperature of measurement in similar way as in Fig. 3. Moreover, the hysteresis loop recorded above the Curie point of the amorphous matrix (Fig. 5, curve c) shows ferromagnetic behaviour of the second (i.e., crystalline) phase present in the sample.

Coercivity versus temperature for the as-quenched and irradiated $\text{Fe}_{81}\text{Mo}_8\text{Cu}_1\text{B}_{10}$ material is presented in Fig. 6. The coercivity of the irradiated sample is higher at tem-

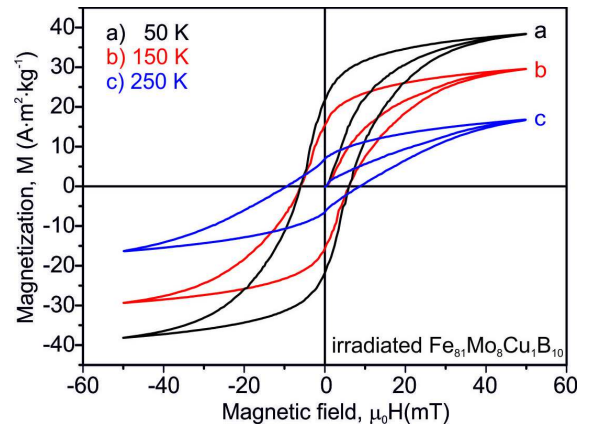


Fig. 5. Hysteresis loops for the $\text{Fe}_{81}\text{Mo}_8\text{Cu}_1\text{B}_{10}$ alloy irradiated with 2×10^{16} ions/ cm^2 measured at the indicated temperatures.

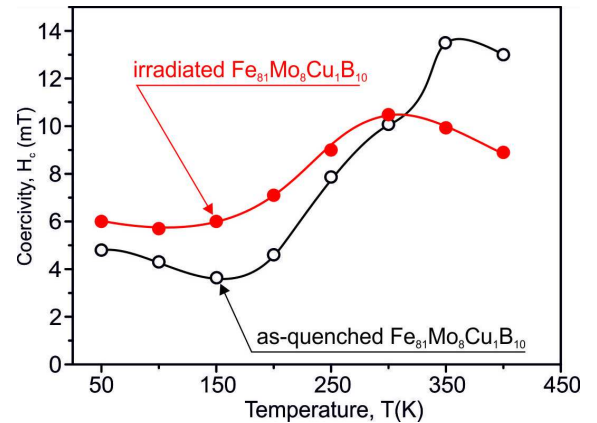


Fig. 6. Temperature dependence of coercivity for the $\text{Fe}_{81}\text{Mo}_8\text{Cu}_1\text{B}_{10}$ alloy in the as-quenched state and after irradiation with 2×10^{16} ions/ cm^2 .

peratures below 300 K. At higher temperatures, the opposite tendency is observed. Moreover, both samples show low and high temperature magnetic hardening which is shifted towards higher temperatures for the as-quenched sample.

4. Conclusions

Effects of ion irradiation upon microstructural and magnetic properties of the $\text{Fe}_{81}\text{Mo}_8\text{Cu}_1\text{B}_{10}$ metallic glass were investigated. Surface features were analysed by CEMS and CXMS techniques while bulk characteristics of the ribbons were followed by magnetic measurements. Presence of structural components comprising amorphous and crystalline regions was confirmed. The latter were identified by Mössbauer effect techniques as *bcc*-Fe, Fe_3O_4 , and nitrides that were formed by ion irradiation.

Acknowledgments

Financial support of the grants VEGA 1/0182/16 and APVV-16-0079 is acknowledged.

References

- [1] M.E. McHenry, M.A. Willard, D.E. Laughlin, *Prog. Mater. Sci.* **44**, 291 (1999).
- [2] K.A. Gschneider, V.K. Pecharsky, A.O. Tsokol, *Rep. Prog. Phys.* **68**, 1479 (2005).
- [3] J. Świerczek, *J. Alloy Comp.* **615**, 255 (2014).
- [4] M. Miglierini, M. Kopcewicz, B. Idzikowski, Z.E. Horváth, A. Grabias, I. Škorvánek, P. Dużewski, Cs.S. Daróczy, *J. Appl. Phys.* **85**, 1014 (1999).
- [5] M. Miglierini, M. Hasiak, *Phys. Stat. Sol. A* **213**, 1138 (2016).
- [6] P. Schaaf, *Prog. Mater. Sci.* **47**, 1 (2002).
- [7] G. Herzer, *IEEE Trans. Magn.* **25**, 3327 (1989).